

CLASSIFIED
SECURITY CLASSIFICATION OF THIS PAGE

MASTER COPY

FOR REPRODUCTION PURPOSES

REPORT DOCUMENTATION PAGE

AD-A207 355

1a. REPORT SECURITY CLASSIFICATION Unclassified		1b. RESTRICTIVE MARKINGS DTIC FILE CO	
2a. SECURITY CLASSIFICATION AUTHORITY		3. DISTRIBUTION / AVAILABILITY OF REPORT Approved for public release; distribution unlimited.	
2b. DECLASSIFICATION / DOWNGRADING SCHEDULE		4. PERFORMING ORGANIZATION REPORT NUMBER(S)	
4. PERFORMING ORGANIZATION REPORT NUMBER(S)		5. MONITORING ORGANIZATION REPORT NUMBER(S) ARO 24620.1-EG-VIR	
6a. NAME OF PERFORMING ORGANIZATION Massachusetts Institute of Technology, Civil Engineering	6b. OFFICE SYMBOL (If applicable) CCRE/PACT	7a. NAME OF MONITORING ORGANIZATION U. S. Army Research Office	
6c. ADDRESS (City, State, and ZIP Code) 77 Massachusetts Avenue, Room 1-175 Cambridge, MA 02139		7b. ADDRESS (City, State, and ZIP Code) P. O. Box 12211 Research Triangle Park, NC 27709-2211	
8a. NAME OF FUNDING / SPONSORING ORGANIZATION U. S. Army Research Office	8b. OFFICE SYMBOL (If applicable)	9. PROCUREMENT INSTRUMENT IDENTIFICATION NUMBER DAAL03-87-K-0005	
8c. ADDRESS (City, State, and ZIP Code) P. O. Box 12211 Research Triangle Park, NC 27709-2211		10. SOURCE OF FUNDING NUMBERS	
11. TITLE (Include Security Classification) Optimum Design Methods for Structural Sandwich Panels		PROGRAM ELEMENT NO.	TASK NO.
12. PERSONAL AUTHOR(S) Gibson, Lorna J.		15. PAGE COUNT 60	
13a. TYPE OF REPORT Technical	13b. TIME COVERED FROM 1/87 TO 12/87	14. DATE OF REPORT (Year, Month, Day) 1 January 1988	
16. SUPPLEMENTARY NOTATION The view, opinions and/or findings contained in this report are those of the author(s) and should not be construed as an official Department of the Army position, policy, or decision, unless so designated by other documentation.			
17. COSATI CODES		18. SUBJECT TERMS (Continue on reverse if necessary and identify by block number)	
FIELD	GROUP	Advanced construction materials; structural composites; sandwich panels.	
19. ABSTRACT (Continue on reverse if necessary and identify by block number)			
Structural sandwich panels are composed of two thin, stiff skins separated by a light weight core. The faces are typically strong materials such as aluminum fiber reinforced composites, while honeycombs or foams are used in the core. The separation of the faces increase the moment of inertia of the panel with minimum increase in weight. Because of this, these panels are extremely efficient in bending and are used in applications where the weight of the member is critical: aircraft, marine, and land vehicles; portable structures; construction in remote areas; roofing shells; and some types of sports equipment (e.g., modern downhill skis). In all of these, the mechanical behavior			
20. DISTRIBUTION / AVAILABILITY OF ABSTRACT <input type="checkbox"/> UNCLASSIFIED/UNLIMITED <input type="checkbox"/> SAME AS RPT. <input type="checkbox"/> DTIC USERS		21. ABSTRACT SECURITY CLASSIFICATION Unclassified	
22a. NAME OF RESPONSIBLE INDIVIDUAL		22b. TELEPHONE (Include Area Code)	22c. OFFICE SYMBOL

DTIC
ELECTE
MAY 01 1989
S
E

Best Available Copy

80
2004 0326 049

UNCLASSIFIED

SECURITY CLASSIFICATION OF THIS PAGE

cont'd

of the sandwich panel depends on the strength and stiffness of the face and the core, on the geometry of the panel (the core and face thicknesses), and on the bond strength between the faces and the core.

Previous optimization studies have centered on defining the best geometry of the panel if the material properties of the face and core, including the core density, are specified. However, recent work on material property-density relationships for foamed core materials now allows the core density to be included as a variable to be optimized. The goal of this research is to determine the core density as well as the core and face thicknesses that minimize the weight of a sandwich panel for given structural requirements. This will improve the minimum weight design of structural sandwich panels in a manner not previously possible. (AW)

Accession For	
NTIS GRA&I	<input checked="" type="checkbox"/>
DTIC TAB	<input type="checkbox"/>
Unannounced	<input type="checkbox"/>
Justification	
By _____	
Distribution/	
Availability Codes	
Dist	Avail and/or Special
A-1	



UNCLASSIFIED

SECURITY CLASSIFICATION OF THIS PAGE

PNO 2280 4000

B

OPTIMUM DESIGN METHODS FOR STRUCTURAL SANDWICH PANELS

ARO PROGRAM IN ADVANCED CONSTRUCTION TECHNOLOGY

FINAL REPORT

L.J. GIBSON
WINSLOW ASSOCIATE PROFESSOR OF CIVIL ENGINEERING
DEPARTMENT OF CIVIL ENGINEERING
MASSACHUSETTS INSTITUTE OF TECHNOLOGY
CAMBRIDGE, MA 02139

1 JANUARY 1988

OPTIMUM DESIGN METHODS FOR STRUCTURAL SANDWICH PANELS

1. Introduction 3

2. Debonding in Foam Core Sandwich Panels.....11

 2.1 Introduction11

 2.2 Analysis13

 2.3 Experimental Method20

 2.4 Results and Discussion22

 2.5 Conclusions25

 2.6 References27

3. Minimum Weight Design of Sandwich Panels
for a Given Strength28

 3.1 Introduction28

 3.2 Analysis29

 3.3 Conclusions45

 3.4 References49

4. Creep of Sandwich Panels50

 4.1 Introduction50

 4.2 Models for Creep in Polymers and Foams50

 4.3 Future Work55

 4.4 References57

5. Conclusions58

6. Appendix - List of symbols59

OPTIMUM DESIGN METHODS FOR STRUCTURAL SANDWICH PANELS

1. Introduction

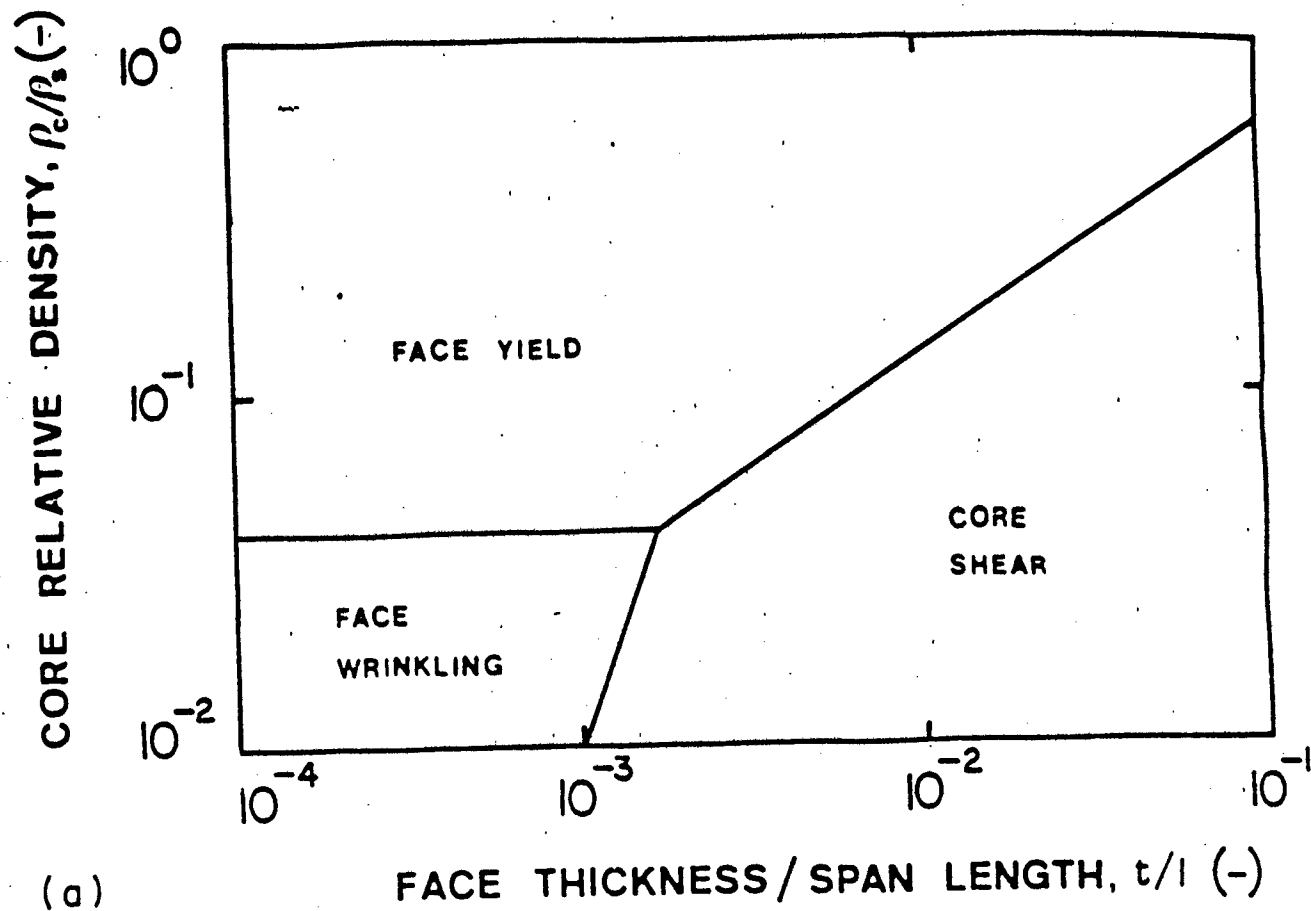
Structural sandwich panels are composed of two thin, stiff skins separated by a lightweight core. The faces are typically strong materials such as aluminum or fibre reinforced composites, while honeycombs or foams are used in the core. The separation of the faces increases the moment of inertia of the panel with minimum increase in weight, giving a panel that is extremely efficient in resisting bending and buckling. Because of this, sandwich panels are used in applications where the weight of the member is critical: in aircraft, marine and land vehicles; in portable structures; in construction in remote areas; in roofing shells; and in some types of sports equipment such as modern downhill skis. Sandwich construction is even found in nature where mechanical design is often optimized: in the skull, two layers of dense, cortical bone are separated by a lightweight core of sponge-like cancellous bone. In each case, the mechanical behaviour of the sandwich panel depends on the strength and stiffness of the face and core materials, on the geometry of the panel and on the strength of the bond between the faces and the core.

The aim of this project has been to find the minimum weight design of a foam core sandwich panel for a given required strength. The optimization analysis for this problem is complicated by the fact that the sandwich may fail by one of several different modes. The face may yield in tension or may

buckle locally in compression (or "wrinkle"). The core may fail in tension, compression or shear. And finally, the bond between the faces and the core may fracture causing delamination. Each of these failure modes is described by a different failure equation. There is not a single, well defined constraint equation for the required strength, then; instead, there is a set of constraint equations. The critical one for a given loading configuration and beam design, occurring at the lowest load, must be determined to carry out the optimization analysis.

Failure mode maps, showing the range of beam designs for which a given failure mode is critical, have been developed in a previous project (Fig. 1.1). Briefly, they are constructed by equating pairs of failure equations in turn to give the equations of the transition lines between failure modes. The failure equations and transition line equations for foam core sandwich beams are given in Tables 1.1 and 1.2; the nomenclature is given in the Appendix to the report. To simplify the development of the failure mode maps, only the failure modes listed in Table 1.1 were considered; in particular, it was assumed that the bond between the faces and the core was perfect and that debonding did not occur.

To proceed with the minimum weight analysis of a foam core sandwich beam we proposed the following tasks for this project:



(a)

Figure 1.1 A failure mode map for a sandwich beam loaded in three-point bending. The beam has aluminum faces and a rigid polyurethane foam core. This map has been made assuming that debonding does not occur.

TABLE 1.1 FAILURE EQUATIONS FOR FOAM-CORE SANDWICH BEAMS

FAILURE MODE	FAILURE EQUATION
Face Yield	$P_{fy} = C_1 \sigma_{yf} bc \frac{t}{\ell}$
Face Wrinkling	$P_{fw} = 0.57 C_1 C_3^{2/3} E_f^{1/3} E_s^{2/3} (\rho_c/\rho_s)^{2/3} bc \frac{t}{\ell}$
Core Yield - Shear	$P_{cs} = \frac{C_4 (\rho_c/\rho_s)^B \sigma_{ys} bc}{\sqrt{\left[\frac{C_3 (\rho_c/\rho_s)^A E_s}{2C_1 (\ell/\ell) E_f} \right]^2 + \left[\frac{1}{C_2} \right]^2}}$
Core Yield-Tension	$P_{ct} = \frac{C_5 (\rho_c/\rho_s)^C \sigma_{ys} bc}{\frac{C_3 (\rho_c/\rho_s)^A E_s}{2C_1 (\ell/\ell) E_f} + \sqrt{\left[\frac{C_3 (\rho_c/\rho_s)^A E_s}{2C_1 (\ell/\ell) E_f} \right]^2 + \left[\frac{1}{C_2} \right]^2}}$
Core-Yield-Compression	$P_{cc} = \frac{C_6 (\rho_c/\rho_s)^E \sigma_{ys} bc}{\frac{C_3 (\rho_c/\rho_s)^A E_s}{2C_2 (\ell/\ell) E_f} + \sqrt{\left[\frac{C_3 (\rho_c/\rho_s)^A E_s}{2C_1 (\ell/\ell) E_f} \right]^2 + \left[\frac{1}{C_2} \right]^2}}$

TABLE 1.2 TRANSITION EQUATIONS FOR FAILURE MODE MAPS

FAILURE MODE	TRANSITION EQUATION
Face yield - Face wrinkling	$\rho_c/\rho_s = \left[\frac{\sigma_{yf}}{0.57 C_3^{2/3} E_f^{1/3} E_s^{2/3}} \right]^{3/2A}$
Face yield - Core shear	$t/c = \frac{C_2 C_4}{C_1} (\rho_c/\rho_s)^B \frac{\sigma_{ys}}{\sigma_{yf}}$
Face wrinkling - Core shear	$t/c = \frac{C_2 C_4}{0.57 C_1 C_3^{2/3}} \left[\frac{\rho_c}{\rho_s} \right]^{B-2A} \frac{\sigma_{ys}}{E_f^{1/3} E_s^{2/3}}$

Note: These transition equations are based on the assumption that normal stresses in the core are insignificant in the core shield failure mode.

(a) Failure Mode Map - Finalize the Debonding Mechanism

The analysis of debonding in sandwich beams is incomplete; to properly understand how debonding and delamination occur requires the application of fracture mechanics to the problem. A crack in the bond will propagate (and cause debonding failure) when the stress field around the crack produces a stress intensity factor equal to the fracture toughness of the adhesive. The analysis of the stress field around the crack is complicated, but a simple dimensional argument can be used to characterize the important parameters in crack propagation. Experimental measurements of the load required to propagate a crack of known length can then be used to calibrate the dimensional analysis to get a more exact description of crack propagation. In these experiments, sandwich beams with deliberate areas of debonding in them, simulating "cracks" will be made. The debonded area can be made by inserting a thin piece of plastic between the face and the core so that no adhesive reaches this area. The crack length is given by the length of plastic strip used. The beams will then be tested in bending to produce a debonding failure; the failure load will be recorded. This will be repeated for different crack lengths. This procedure should allow a complete characterization of the debonding process in sandwich beams.

(b) Optimization Analysis of a Sandwich Beam subject to a Strength Constraint

In this part of the project we will do the optimization analysis for the strength constraint. This can be done by using each failure equation in turn as the constraint equation in the optimization analysis and then comparing all the results to determine the minimum weight solution. This, however, is time consuming and laborious, as the equations may not have closed form solutions. We intend to try to use the information given by the failure map to simplify the optimization procedure; the details will be worked out during this task.

(c) Experimental Verification of the Optimization Analysis

The properties of the foam to be used in the core of the sandwich beams will first be measured so that the exact property-density relationships can be used in the optimization analysis. Then, a series of sandwich beams, of varying weight but constant strength, will be designed, made and tested to failure in bending. Load-deflection plots will be recorded for each beam and the mode of failure noted. We will also take photographs of the failed beams. If the results of the tests agree with the analysis, they will increase confidence in it; otherwise they will be helpful in indicating the deficiencies of the analysis.

The debonding study and the optimization analysis of a sandwich beam subject to a strength constraint have been completed and are described in more detail below in Sections 2

and 3. The experimental verification of the optimization analysis has been omitted as the only tests that could be done would duplicate ones done earlier in another study. Instead, we have begun work on modelling creep in foam core sandwich panels; this work is described in Section 4.

2. Debonding in Foam Core Sandwich Panels

2.1. Introduction

Structural members made up of two stiff, strong skins separated by a lightweight core are known as sandwich panels. The separation of the skins by the core increases the moment of inertia of the panel with little increase in weight, producing an efficient member for resisting bending and buckling loads. The low weight of sandwich panels was first exploited by the aircraft industry; ultra-light panels using carbon fibre-composite skins and honeycomb cores are now used routinely in modern aerospace components. Sandwich panel technology is now being transferred to building applications such as roof and wall panels; the cores of such panels are typically made of foam to give good thermal insulation in addition to low weight.

It is critical that the bond between the skins and the core remain intact for the panel to perform satisfactorily. In this paper, we describe the criterion for debonding in a sandwich beam with isotropic faces and a foam core in terms of the critical strain energy release rate. Tests on sandwich beams with aluminum skins and foamed polyurethane cores show that the analysis describes debonding failure well. Comparison of the load for debonding with that for other modes of failure, such as face yielding, face wrinkling and core shearing, show that debonding occurs only if there are relatively large pre-existing cracks at the interface; otherwise it is preceded by another mode of failure. The results are useful in determining the maximum

permissible interface crack for a sandwich panel with a foam core.

The propagation of a crack at the interface between two dissimilar elastic media has been studied by several workers. England [1] calculated the stress intensity factor for normal loading of an interface crack between two dissimilar elastic media; this solution suffers from the difficulty that it requires the two materials to wrinkle and overlap near the ends of the crack which is physically unrealistic. Comninou [2-4] reexamines England's solution and finds that if a frictional contact zone is introduced at the ends of the crack, a more realistic solution is possible. She calculates the stress intensity factor for both normal [2,3] and shear [4] loading. The difficulty with such analyses is that they are difficult to implement as the size of the frictional zone ahead of the crack tip must be estimated. Other workers, concerned with debonding in fibre composite laminates, have examined a more complex crack geometry with a through crack in one layer running into a perpendicular interface crack between that layer and the next [5-9]; these analyses use a complex variable formulation to reduce the problem to a set of integral equations which are solved numerically. Here, we treat the problem of the propagation of an interface crack in a sandwich panel with isotropic faces and a foamed core in a simpler manner, by examining the strain energy release rate required for crack propagation and measuring the critical strain

energy release rate of the interface experimentally.

2.2. Analysis

Consider the sandwich beam shown in Fig. 2.1 of stiffness, S . It has a length, l , a width, b , and face and core thicknesses, t and c . The density and Young's modulus of the core and face materials are ρ_c , ρ_f , E_c and E_f . The flexural rigidity of the beam is given by [10]:

$$D = \frac{E_f b t^3}{6} + \frac{E_f b t d^2}{2} + \frac{E_c b c^3}{12} \quad (1)$$

where $d = c + t$. The stiffness of the beam is [10]:

$$S = \frac{P}{\delta} = \frac{P}{\frac{P l^3}{C_1 D} + \frac{P l}{C_2 A_e G_c}} = \frac{C_1 C_2 A_e G_c D}{C_2 l^3 A_e G_c + C_1 l D} \quad (2)$$

where $A_e (=bd^2/c)$ is an equivalent core area and C_1 and C_2 are constants relating to the loading geometry. For example, for a simply supported beam under three-point bending, $C_1 = 48$ and $C_2 = 4$.

The beam contains a crack of length $2a$ at the interface between the face and core and is loaded by a concentrated load, P . We now determine the load, P , which causes the crack to propagate by examining the strain energy release rate. The

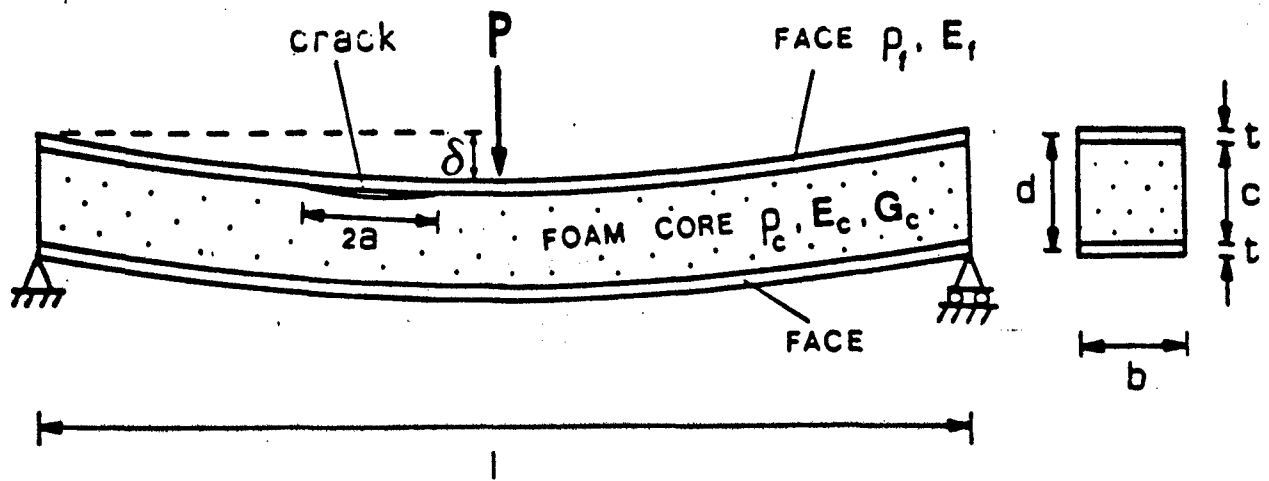


Fig. 2.1 The geometry of a sandwich beam with an interfacial crack of length $2a$.

elastic energy in a perfectly bonded beam is:

$$U = \frac{1}{2} P \delta = \frac{1}{2} \frac{P^2}{S} \quad (3)$$

and the energy per unit volume, if the faces are thin compared to the core, is

$$\frac{U}{V} = \frac{1}{2} \frac{P^2}{S b' c} \quad (4)$$

If $a > c$, the volume unloaded by a crack of length a is $2abc$ (Fig.2.2a) and the corresponding released energy is:

$$U(a) = - \frac{1}{2} \frac{P^2}{S b' c} 2abc = - \frac{P^2 a}{S} \quad (5)$$

The mode II strain energy release rate, G_{IIc} , for in-plane shear delamination is given by:

$$G_{II} = - \frac{1}{b} \frac{\partial U(a)}{\partial a} \quad (6)$$

so that

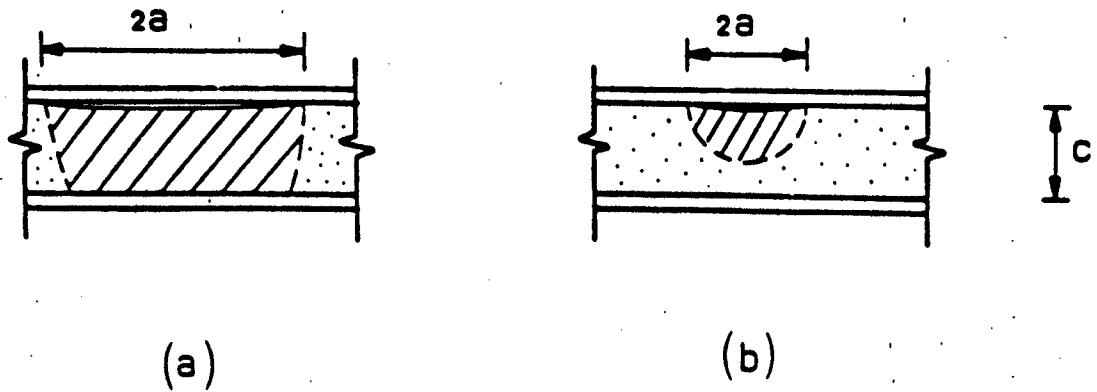


Fig. 2.2 (a) The unloaded volume for a crack half length greater than the depth of the core.
(b) The unloaded volume for a crack half length less than the depth of the core.

$$G_{II} = \frac{P^2}{Sb^2} \quad (7)$$

Fracture occurs when the strain energy release rate, G_{II} , equals the critical strain energy release rate for the interface, G_{IIC} :

$$G_{II} = G_{IIC} \quad (8)$$

which gives the failure load

$$P = \sqrt{Sb^2 G_{IIC}} \quad (9)$$

If the crack length is smaller than the beam thickness, c , the unloaded volume is roughly $\frac{1}{2} a^2 b$ (Fig. 2.2b) and the same procedure gives:

$$P = \sqrt{\frac{2S b^2 c G_{IIC}}{\pi a}} \quad (10)$$

Experimental evidence shows that debonding is not likely to occur unless a large crack exists at the interface (in which case equation (9) gives the debonding load).

The critical strain energy release rate of the interface, G_{IIC} , can be found from shear tests. Consider the double-shear specimen shown in Fig. 2.3. The elastic energy in the specimen is:

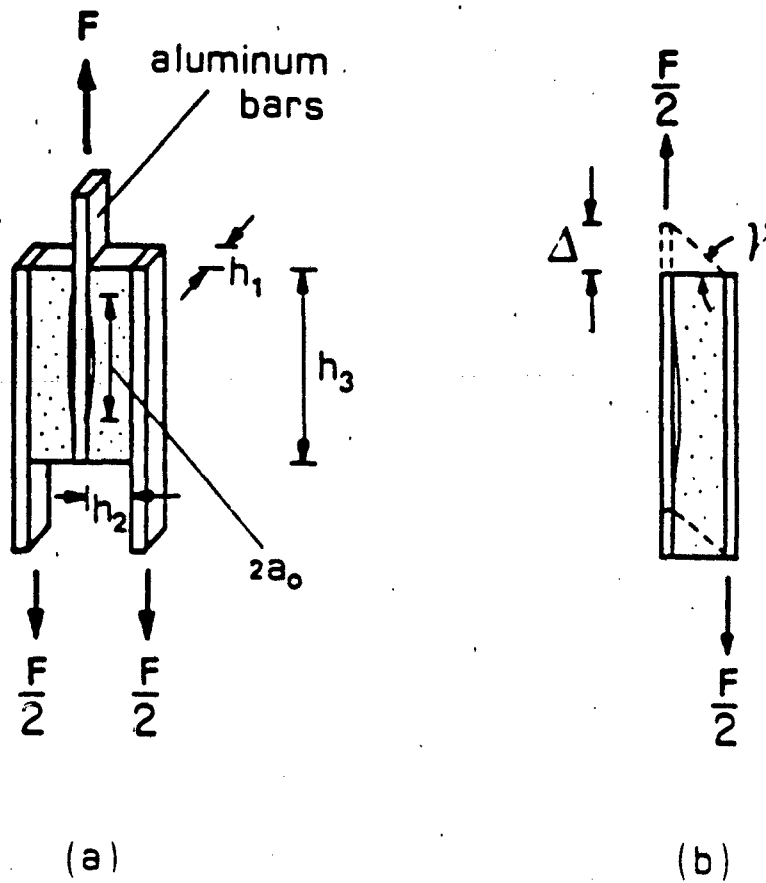


Fig. 2.3 (a) The double-shear test specimens used to measure the critical strain energy release rate of the interface.
 (b) The loading on one half of the double-shear specimen.

$$U = \frac{F\Delta}{4} \quad (11)$$

with (for small strains)

$$\Delta = \tau h_2 = \frac{\tau}{G_c} h_2 \quad (12)$$

so that

$$U = \frac{F \tau}{4 G_c} h_2 \quad (13)$$

where F is the applied load, τ is an average shear stress on the face with the crack, h_2 is the depth of the specimen and G_c is the shear modulus of the core. The average shear stress can be approximated as

$$\tau = \frac{F}{2h_1(h_3 - 2a_0)} \quad (14)$$

where h_3 is the length of the specimen and a_0 is the crack length at the foam-plate interface. It follows that the energy per unit volume can be written as

$$\frac{U}{V} = \frac{F^2}{8G_c h_1^2 h_3 (h_3 - 2a_0)} \quad (15)$$

The energy released by a crack of length $2a_0$ ($a_0 > h_2$) is

approximated as

$$U(a_0) = - \frac{2F a_0 h_1 h_2}{8G_C h_1^2 h_3 (h_3 - 2a_0)} = - \frac{F^2 a_0 h_2}{4G_C h_1 h_3 (h_3 - 2a_0)} \quad (16)$$

and the strain energy release rate is

$$G_{II} = - \frac{1}{h_1} \frac{\partial U(a_0)}{\partial a_0} = \frac{F^2 h_2}{4G_C h_1^2 (h_3 - 2a_0)^2} \quad (17)$$

At failure of the specimen (delamination)

$$G_{IIC} = \frac{F_d^2 h_2}{4G_C h_1^2 (h_3 - 2a_0)^2} \quad (18)$$

where F_d is the load for delamination. Equation (18) can be used for the evaluation of the critical strain energy release rate for each foam density.

2.3. Experimental Method

The critical strain energy release rate for the interface was measured using double shear specimens pulled in tension (Fig 2.3). The aluminum faces and rigid polyurethane foam cores of densities 64, 96, 160, 192 and 320 kg/m³ were bonded together with a polyester resin adhesive. The dimensions of the specimens were: $h_1 = 25.4$ mm, $h_2 = 9.5$ mm (64 and 96 kg/m³ specimens), $h_2 = 12.7$ mm (160, 192 and 320 kg/m³ specimens) and $h_3 = 76.2$ mm. Cracks of length 31.8, 38.1 and 50.8 mm were introduced into the interface by not applying the adhesive to the area of the crack

and by inserting a removable plastic strip into the crack while the specimens were pressed together and cured. The specimens were loaded in tension in Instron testing machine and the load and deflection recorded. Three specimens of each crack length and density were tested. Debonding did not occur in the 64 and 96 kg/m³ density foam specimens even when the crack length was two thirds of the length of the specimen; instead these specimens failed by plastic shearing of the foam. The 160, 192 and 320 kg/m³ specimens failed by crack propagation along the interface. In the case of the 160 and 192 kg/m³ specimens, the crack propagated through the foam adjacent to the interface, while in the 320 kg/m³ specimens it propagated within the adhesive layer. The load deflection behaviour was linear to failure for all three densities.

The shear moduli of the foams were measured on double shear specimens with no interface crack. The dimensions of the specimens were $h_1 = 25.4$ mm, $h_2 = 9.5$ mm and $h_3 = 76.2$ mm. The specimens were loaded in tension and were linear elastic.

A set of sandwich beams was made by bonding aluminum skins to rigid foamed polyurethane cores with polyester resin. Interface cracks of known length were introduced by the same method as in the critical strain energy release rate tests. A range of beam designs were tested. The beams were loaded to failure in three point bending using a screw jack. Load and deflection were measured during the test with a load cell and a

LVDT and were recorded on an X-Y recorder. The beams were linear-elastic to failure which was by crack propagation along the interface through the foam.

2.4 Results and Discussion

The critical strain energy release rate was calculated from the double shear tests using equation (18); the results are given in Table 2.1 for each of the foam densities tested for which debonding occurred. G_{IIc} is independent of the length of the crack along the interface. For the two lower density foams for which the crack propagated through the foam along the interface, G_{IIc} corresponds to the surface energy of the foam at the interface. The largest value of G_{IIc} , for the 320 kg/m³ foam for which the crack propagated through the adhesive, corresponds to the surface energy of the adhesive. There is a transition from crack propagation in the foam to crack propagation in the adhesive at a foam density between 192 and 320 kg/m³.

The failure modes and loads of the sandwich beams are listed in Table 2.2 along with the expected load for debonding failure (equation (9) or (10), depending on the crack length). The beams with interfacial cracks which are large relative to the core thickness, c , failed by debonding. There is a slight dependence of the failure load on the crack length, $2a$, with the debonding load decreasing by about 5% as the crack length increases from 127 mm to 204 mm. The agreement between the measured and

TABLE 2.1. CRITICAL STRAIN ENERGY RELEASE RATES OF THE FOAMS

Core density, ρ_c (kg/m ³)	Crack length, $2a_0$ (mm)	Measured failure load, F_d (N)	Calculated G_{Ic} (J/m ²) (eqn 18)	Mean G_{Ic} (J/m ²)
160	31.8	3150	1530	1560
	38.1	2840	1690	
	50.8	1760	1460	
192	31.8	4130	1580	1630
	38.1	3670	1690	
	50.8	2390	1610	
320	31.8	5480	2000	1900
	38.1	4600	1910	
	50.8	2960	1780	

Notes

1. For all specimens $h_1 = 25.4$ mm, $h_2 = 12.7$ mm, $h_3 = 76.2$ mm.
2. The shear moduli of the foams were 16.2, 27.0 and 37.5 MN/m² for the 160, 192 and 320 kg/m³ densities, respectively.
3. The measured failure loads are the average of 3 tests.

TABLE 2.2 FAILURE LOADS OF TEST BEAMS.

l (mm)	2a (mm)	c (mm)	t (mm)	b (mm)	ρ_c (kg/m ³)	P _{fail} (N)	Mode	P (N) (eqn 9 or 10)
381	127	51	3.18	38	160	3150	debonding	3030
381	152	51	3.18	38	160	3090*	debonding	2990
381	204	51	3.18	38	160	2830*	debonding	2930
381	127	51	3.18	38	192	3980	debonding	3820
381	152	51	3.18	38	192	3910*	debonding	3785
381	204	51	3.18	38	192	3810*	debonding	3730
381	127	51	3.18	38	320	5420	debonding	4890
381	152	51	3.18	38	320	5310*	debonding	4850
381	204	51	3.18	38	320	5190*	debonding	4790
508	127	51	3.18	38	160	2910	debonding	3110
508	152	51	3.18	38	160	2780*	debonding	3070
508	204	51	3.18	38	160	2650*	debonding	2980
508	127	51	3.18	38	192	3790	debonding	3910
508	152	51	3.18	38	192	3720*	debonding	3870
508	204	51	3.18	38	192	3670*	debonding	3800
508	127	51	3.18	38	320	4860	debonding	5020
508	152	51	3.18	38	320	4750*	debonding	4980
508	204	51	3.18	38	320	4670*	debonding	4930
241	50	25	1.27	25	160	1100	face yield	890
241	76	25	1.27	25	160	1090	face yield	1105
241	76	25	1.27	25	320	1120	face yield	5450
267	38	25	0.63	25	160	470	face yield	650
267	38	25	0.63	25	320	490	face yield	1490

Note

Failure loads marked by an asterisk are the average of 2 tests; otherwise, they are the result of 3 tests.

calculated debonding loads is within 10% for all beam geometries and crack lengths. The analysis describes debonding in sandwich beams with foam cores well.

The beams with relatively small interfacial cracks yielded before debonding occurred; for these beams the predicted debonding load is greater than the measured face yielding load with only one exception, for which the yield and debond loads are similar. Similar calculations for a wide range of sandwich beams indicate that debonding is usually preceded by another failure mode (eg. face yielding, face wrinkling or core shearing) if the interfacial crack is small relative to the core thickness.

Triantafillou and Gibson [11] have recently analyzed the various failure modes of aluminum skin - rigid polyurethane foam core sandwich beams; the usual modes of failure are face yielding, face wrinkling and core shear. By comparing the failure load for each of these modes with that for debonding it is possible to determine whether or not debonding is the critical failure mode for a particular sandwich design.

2.5. Conclusions

Debonding in sandwich panels with foam cores can be described in terms of the critical strain energy release rate of the interface. The results of the analysis describe the measured debonding load in sandwich beams with aluminum skins and rigid polyurethane foam cores well. They suggest that debonding is unlikely to occur unless the initial interfacial crack length is

relatively large. The debonding failure load given by the analysis presented here can be compared with the failure loads for other modes such as face yielding, face wrinkling and core shearing to determine if debonding is the critical failure mode for a given beam geometry and initial crack length.

2.6 References

- [1] England, A.H. (1965) J. Appl. Mech. 32, 400-402.
- [2] Comninou, M. (1977a) J. Appl. Mech. 44, 631-636.
- [3] Comninou, M. (1977b) J. Appl. Mech. 44, 780-781.
- [4] Comninou, M. (1978) J. Appl. Mech. 45, 287-290.
- [5] Erdogan, F. and Arin, K. (1972) Eng. Fract. Mech. 4, 409-458.
- [6] Ko, W.L. (1978) Eng. Fract. Mech. 10, 15-23.
- [7] Ratwani, M.M. (1978) AAIA J. 17, 988-994.
- [8] Hong, C.S. and Ro, H.S. (1981) Int. J. Fracture 17, 181-184.
- [9] Hong, C.S. and Jeong, K.Y. (1985) Eng. Fract. Mech. 21, 285-292.
- [10] Allen, H.G. (1969) Analysis and Design of Structural Sandwich Panels Pergamon Press, Oxford.
- [11] Triantafillou, T.C. and Gibson, L.J. (1987) Mat. Sci. and Eng., 95, 37-53.

3. Minimum Weight Design of a Sandwich Panel for a Given Strength

3.1. Introduction

The goal of this part of the project is to find the minimum weight design of a foam core sandwich beam for a given strength. The optimum value of three design variables are to be found in the analysis: the face thickness, t , the core thickness, c , and the core density, ρ_c . The use of previously developed models for the behaviour of the foam core which relate the properties of a foam to its relative density [1-3] allows the core density to be included as a design variable for the first time. The analysis presented in this section of the report is for a sandwich beam with aluminum faces and a rigid polyurethane foam core loaded in three-point bending. It is easily adapted to other face and core materials and other loading conditions using the method outlined below.

The possible failure modes which will be considered are face yielding, face wrinkling and core shearing. The results of the first part of this study indicate that debonding is only possible if very large cracks (larger than the core thickness) preexist in the interfaces between the faces and the core; we assume here that no such large cracks are present in the interfaces.

3.2 Analysis

Strength contours may be superimposed on failure mode maps by using the failure equations listed in Table 1.1 (Fig. 3.1) [4]. They indicate that the minimum weight design for a sandwich panel occurs at the transition between one failure mode and another. For example, within the regime of face yielding, the core density can be reduced to that corresponding to the transition between face yielding and face wrinkling with no change in strength. Similarly, within the regime of core shear, the face thickness can be reduced to that corresponding to simultaneous core shearing and face yielding with no loss of strength. For each transition between two failure modes, a minimum weight design can be found by using the equation for the weight of the sandwich as the objective function to be minimized and by using the two failure equations for the modes under consideration as the constraint equations. Two of the design variables (the face and core thicknesses and the core density) are solved for in terms of the constraint equations and substituted into the weight equation. Setting the derivative of the weight equation equal to zero then gives the minimum weight design. The results of the analysis for each of the transitions between failure modes are given in Table 3.1a for the general case and in Table 3.1b for a sandwich beam with aluminum faces and a polyurethane foam core loaded in three point bending.

It remains to identify which transition between failure modes corresponds to the overall minimum weight design for a

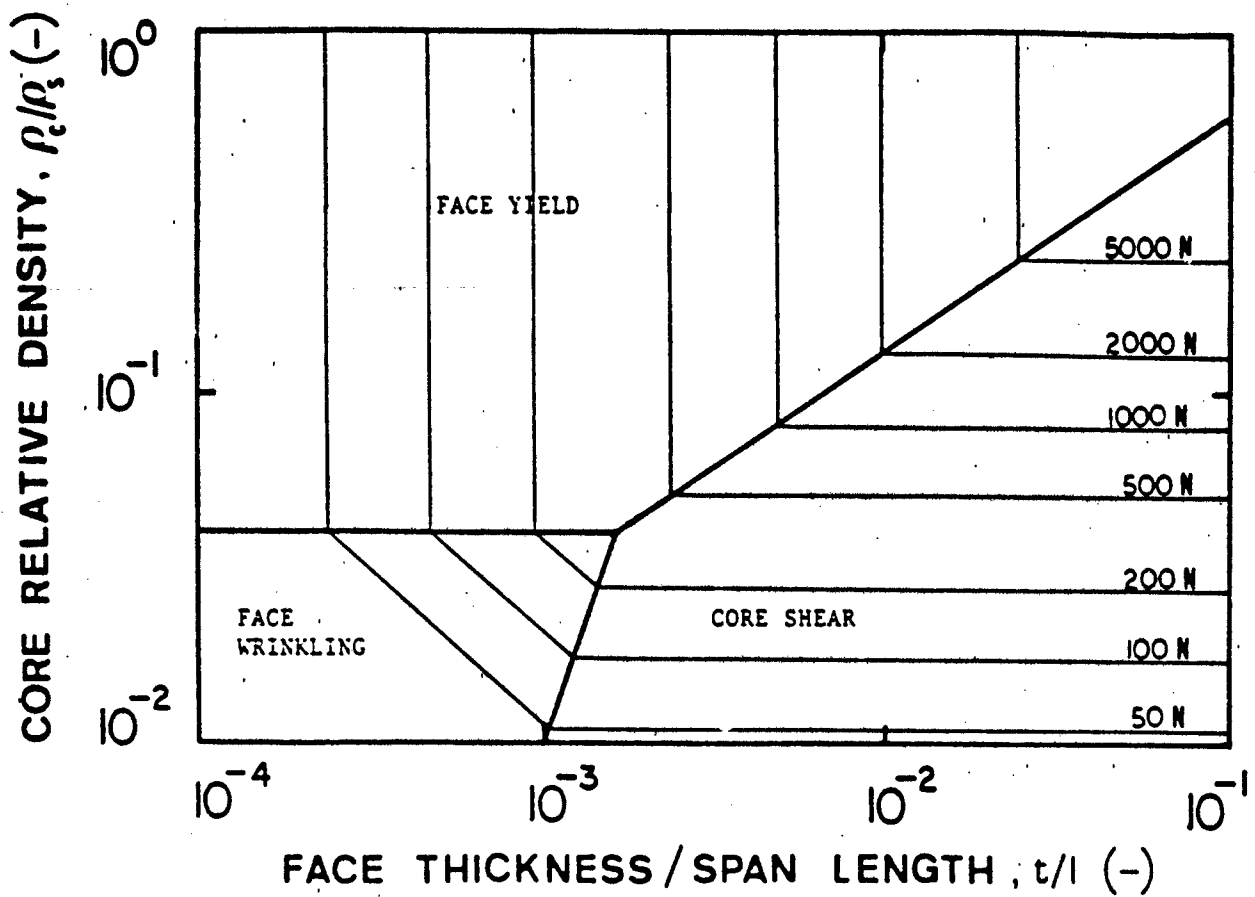


Figure 3.1 A failure mode map for a sandwich beam loaded in three-point bending with strength contours superimposed on the map. The map is for a beam with aluminum faces and a rigid polyurethane foam core.

Table 3.1a Minimum Weight Design of Sandwich Beams for Each Transition Between Failure Modes

Face Yielding/Face Wrinkling

$$c_{opt} = \left[\frac{2 \rho_f P \ell a^{3/2A}}{C_1 \rho_s (\sigma_{yf})^{1+\frac{3}{2A}} b} \right]^{1/2}$$

$$t_{opt} = \frac{P \ell}{C_1 \sigma_{yf} b c_{opt}}$$

$$(\rho_c/\rho_s)_{opt} = \left[\frac{\sigma_{yf}}{a} \right]^{3/2A}$$

$$a = 0.57 C_3^{2/3} E_f^{1/3} E_s^{2/3}$$

Face Yielding/Core Shear

$$c_{opt} = \left[\frac{2B}{C_1(B-1)} \frac{\rho_f}{\rho_s} \frac{P^{B-1} \ell}{\sigma_{yf}} (C_2 C_4 \sigma_{ys})^{1/B} \right]^{\frac{B}{2B-1}}$$

Face

$$t_{opt} = \frac{P l}{C_1 \sigma_{yf} c_{opt} b}$$

$$(\rho_c / \rho_s)_{opt} = \left[\frac{P}{C_2 C_4 \sigma_{ys} c_{opt} b} \right]^{1/B}$$

Face Wrinkling/Core Shear

$$c_{opt} = \left[\frac{-\frac{\rho_s}{\rho_f} \left[\frac{3B-3}{4A-6B} \right] \frac{C_1 \alpha}{(C_2 C_4 \sigma_{ys})^{2A+3}} \frac{(P/b)}{t} \frac{3-3B+2A}{3B}}{\frac{3B}{2A-6B}} \right]$$

$$t_{opt} = \frac{P l}{C_1 \alpha (\rho_c / \rho_s)^{2A/3} c_{opt} b}$$

Note:

$$(\rho_c / \rho_s)_{opt} = \left[\frac{P}{C_2 C_4 \sigma_{ys} c_{opt} b} \right]^{1/B}$$

$$\alpha = 0.57 C_3^{2/3} E_f^{1/3} E_s^{2/3}$$

Table 3.1b Minimum Weight Design of Sandwich Beams for Each Transition Between Failure Modes

Face Yielding / Face Wrinkling

$$t_{opt} = 0.0050 (P/bl)^{0.5} l \quad t/l < 0.00164$$

$$c_{opt} = 0.5801 (P/bl)^{0.5} l \quad P/bl < 0.107$$

$$(\rho_c/\rho_s)_{opt} = 0.0389$$

Face Yielding / Core Shear

$$t_{opt} = 0.0039 (P/bl)^{0.146} l \quad t/l > 0.00164$$

$$c_{opt} = 0.7470 (P/bl)^{0.255} l \quad P/bl > 0.315$$

$$(\rho_c/\rho_s)_{opt} = 0.0685 (P/bl)^{0.49} \quad \rho_c/\rho_s > 0.0389$$

Face Wrinkling / Core Shear

$$t_{opt} = 0.0048 (P/bl)^{0.422} l \quad t/l < 0.00164$$

$$c_{opt} = 0.0241 (P/bl)^{-0.69} l \quad P/bl < 0.079$$

$$(\rho_c/\rho_s)_{opt} = 0.6556 (P/bl)^{1.111} \quad \rho_c/\rho_s < 0.0389$$

Face Yielding / Face Wrinkling / Core Shear

$$t_{opt} = 0.00164 l$$

$$c_{opt} = 1.7683 (P/bl) l$$

$$(\rho_c/\rho_s)_{opt} = 0.3887$$

Notes

1. This table was obtained using the equations from Table 3.1a with the values of the material properties for aluminum faces and a rigid polyurethane foam core. They are:

$$\begin{array}{lll} \rho_f = 2700 \text{ kg/m}^3 & \rho_s = 1200 \text{ kg/m}^3 & C_1 = 4 & A = 1.71 \\ E_f = 70 \text{ GN/m}^2 & E_s = 1.6 \text{ GN/m}^2 & C_2 = 2 & B = 1.52 \\ \sigma_{yf} = 86 \text{ MN/m}^2 & \sigma_{ys} = 127 \text{ MN/m}^2 & C_3 = 1.13 & \\ & & C_4 = 0.31 & \end{array}$$

2. P/bl is in MN/m^2 ; t , c , and l are in m .

given required strength. This is done by comparing the minimum weight for each transition between failure modes for a range of given strengths; the results are shown in Table 3.2 for the aluminum face-polyurethane core sandwich beam. Note that the minimum weight design for a particular transition must fall within the feasible region of the transition it corresponds to; otherwise it is not a valid failure mode. We find that for any given P/bl (the required strength per unit width per unit length) one transition gives the absolute minimum weight design and that the transitions are:

$P/bl < 0.107 \text{ MN/m}^2$ Face yielding / Face wrinkling
 $0.107 < P/bl < 0.315 \text{ MN/m}^2$ Face yielding / Face wrinkling / Core shear
 $P/bl > 0.315 \text{ MN/m}^2$ Face yielding / Core shear

Having identified the failure modes which give the minimum weight beam for a given strength, the weight of the optimal beam can be plotted against strength (Fig. 3.2). The design variables (the face and core thicknesses, t and c , and the core density, ρ_c) can be found using Table 3.1 for the appropriate transition. For the aluminum face-polyurethane core sandwich beam, the optimum beam dimensions are plotted in Fig. 3.3 as a function of the required strength of the beam per unit width and length, P/bl . It is interesting to note that the optimum relative density of the core is between 0.04 and 0.06 for P/bl up to 0.7 MN/m (or 100 psi), corresponding to densities between 3 and 4.5

Table 3.2 Comparison of Minimum Weight as a Function of Strength for Transitions Between Failure Modes

Minimum Mass per (Length)², w_{min} / gl^2 (kg/m²)

P/bl (MN/m ²)	FY/FW	FY/FW/CS	FY/CS	FW/CS
0.01	<u>5.405</u>	9.682	NV	6.473
0.05	<u>11.990</u>	12.979	NV	12.915
0.10	<u>17.195</u>	<u>17.103</u>	NV	NV
0.15	NV	<u>21.226</u>	NV	NV
0.20	NV	<u>25.354</u>	NV	NV
0.30	NV	<u>33.601</u>	NV	NV
0.40	NV	41.847	<u>41.813</u>	NV
0.50	NV	50.099	<u>49.079</u>	NV
0.60	NV	58.345	<u>56.525</u>	NV
0.70	NV	66.592	<u>63.265</u>	NV

Notes

1. The underlined values are the overall minimum weight designs for each P/bl.
2. NV = not a valid failure mode (the optimum design given by the equations of Table 3.1 for this failure mode lies outside of the feasible region of the mode).

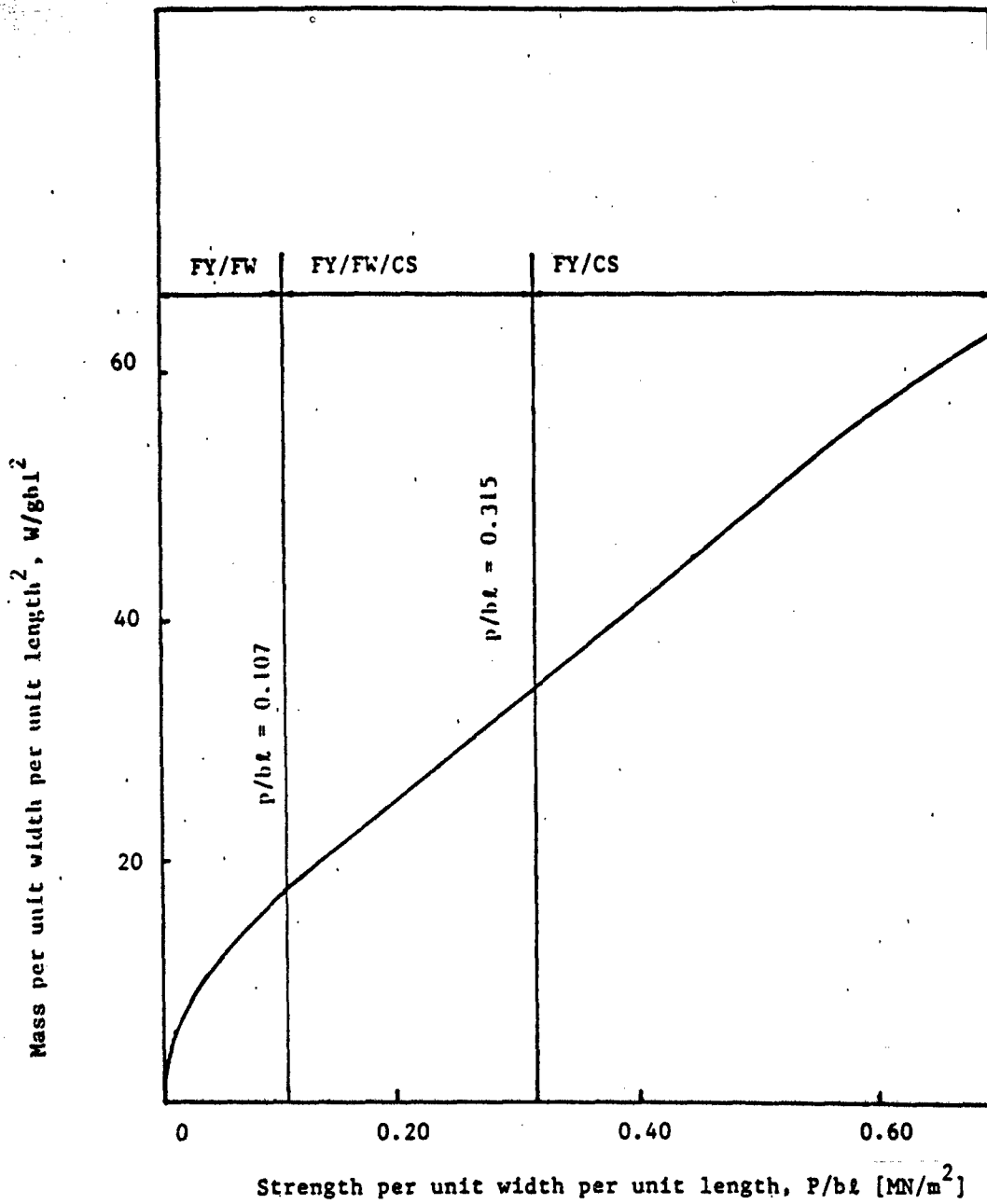


Figure 3.2 The minimum weight per unit width per unit length² as a function of the required strength per unit width per unit length. The plot is for a sandwich beam with aluminum faces and a rigid polyurethane foam core loaded in three point bending.

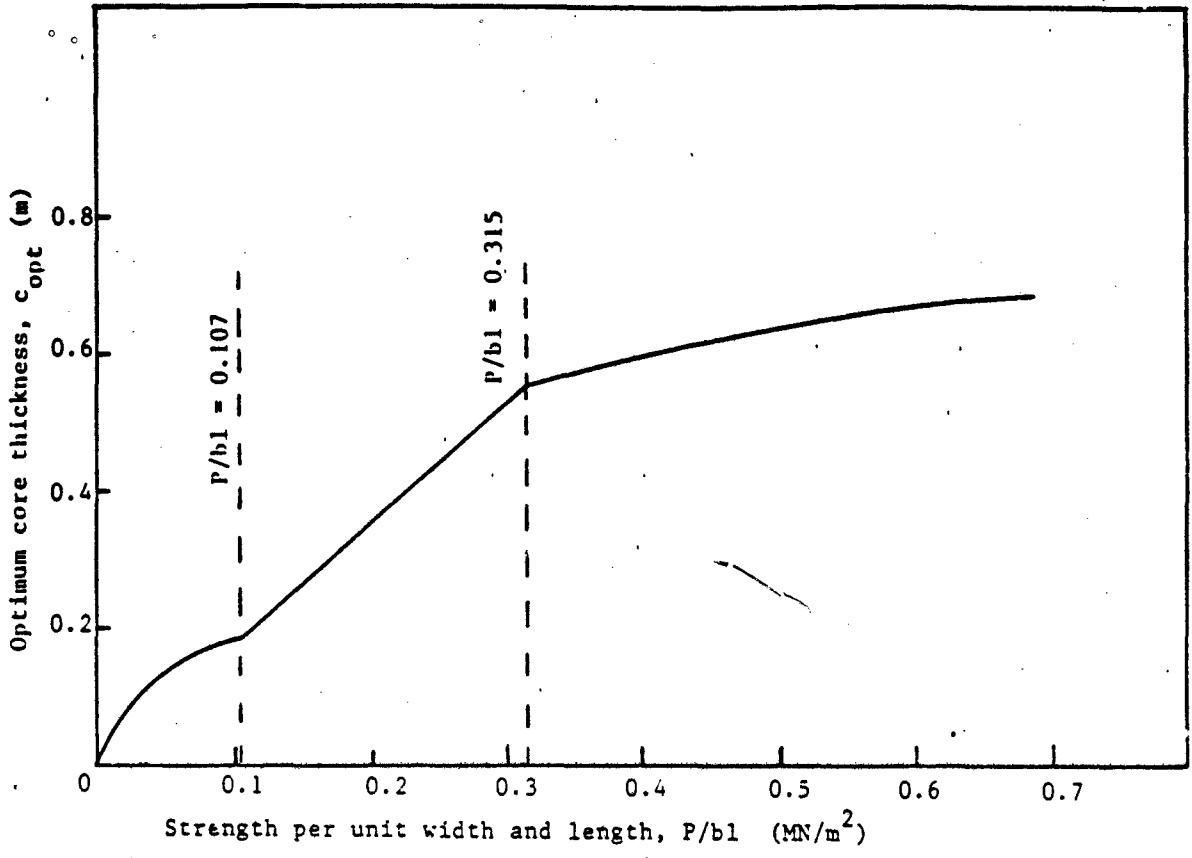


Fig. 3.3 a Optimum core thickness as a function of required strength per unit width and length for a sandwich beam with aluminum faces and a rigid polyurethane foam core loaded in three-point bending.

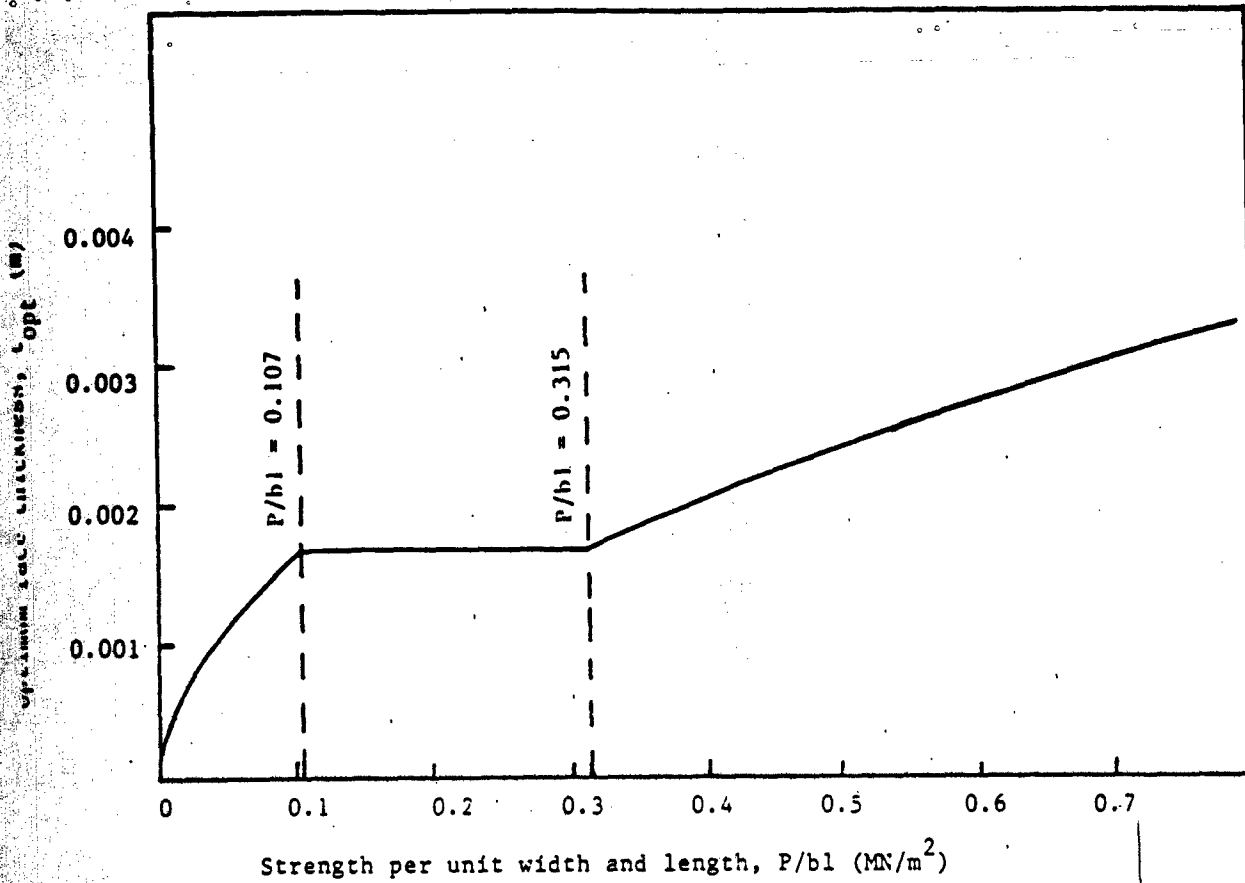


Fig. 3.3 b Optimum face thickness as a function of required strength per unit width and length for a sandwich beam with aluminum faces and a rigid polyurethane foam core loaded in three-point bending.

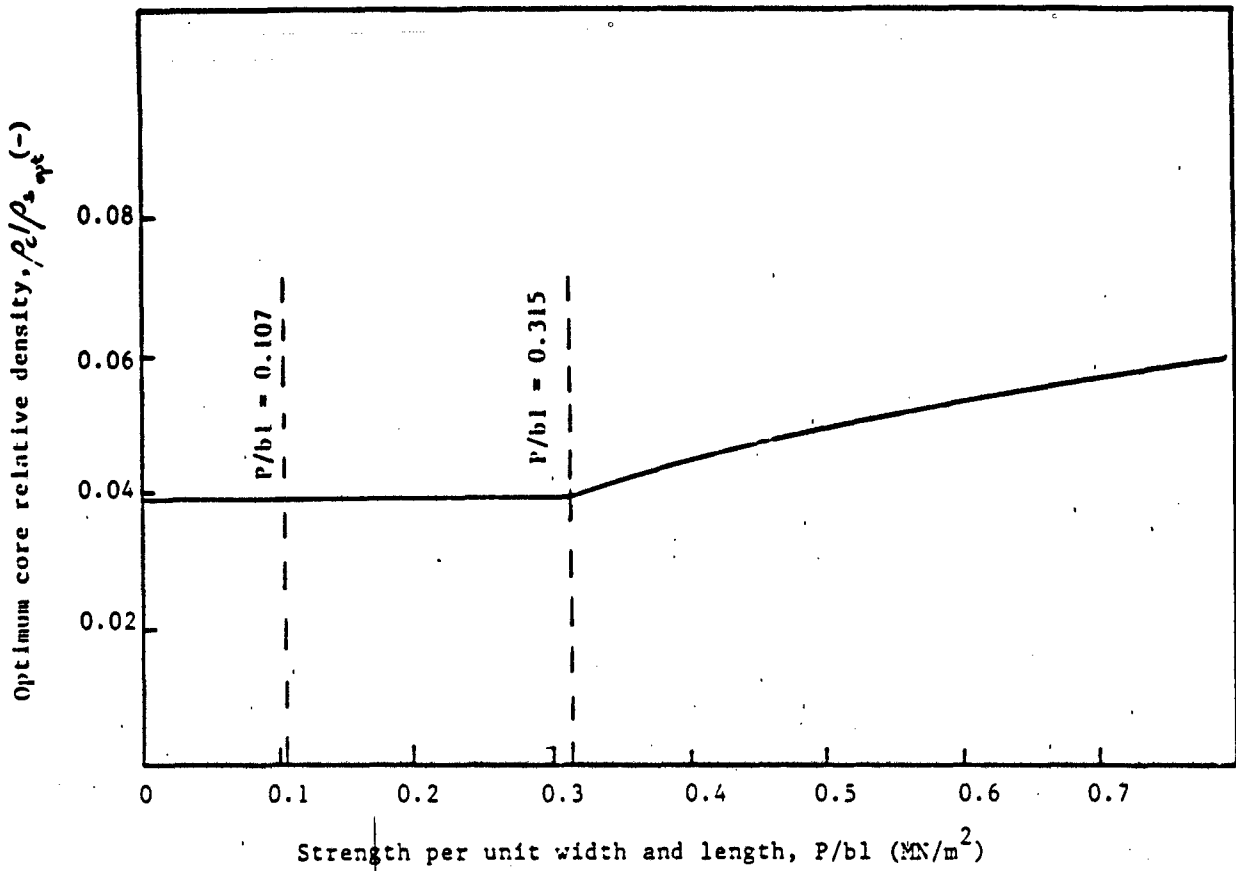


Fig. 3.3 c Optimum core relative density as a function of required strength per unit width and length for a sandwich beam with aluminum faces and a rigid polyurethane foam core loaded in three-point bending.

pounds per cubic foot. The thermal conductivity of foams is lowest at these densities, so that the minimum weight design also optimizes the thermal performance of the panel.

A series of minimum weight beams for various P/bl , corresponding to the line in Fig. 3.2 have been designed. For one value of weight for each transition between failure modes, a series of sandwich beams has been designed. For a given P/bl (and weight) the optimum values of the design variables, t , c and ρ are found. A series of beams with the same weight as the optimum but with different strengths were designed by holding the core density at its optimum value and varying t and c . This process was repeated, holding each design variable constant at its optimum value in turn, for each of the transitions between failure modes. The beam designs for the transition between face yielding and core shear failure had unreasonably large core thicknesses. They were reduced by redesigning the beams for face yield failure only; to do this, slightly higher core densities than those corresponding to the transition between face yielding and core shearing were used. The resulting beam designs are given in Table 3.3 and a plot of the strength per unit weight of these beams (Fig. 3.4) shows the maxima corresponding to the minimum weight designs.

In a previous study [4] the failure equations for each mode of failure described here were confirmed experimentally on sandwich beams with aluminum faces and rigid polyurethane foam cores loaded in three-point bending. In addition, the failure

Table 3.3 Beam Geometries

Transition Between Face Yielding and Face Wrinkling

$W = 5.22 \text{ N}$ $l = 1.0 \text{ m}$ $b = 0.05 \text{ m}$

$t_{opt} = 0.00102 \text{ m}$ $c_{opt} = 0.107 \text{ m}$ $\rho_{t_{opt}} = 48 \text{ kg/m}^3$ $P/bl = 0.039 \text{ MN/m}^2$

$t \text{ (m)}$	$\rho_c \text{ (kg/m}^3)$	$c \text{ (m)}$	$P/bl \text{ (MN/m}^2)$	$W \text{ (N)}$
0.00102	48	0.107	0.039	5.22
0.00102	16	0.322	0.033	5.22
0.00102	32	0.161	0.037	5.22
0.00102	64	0.080	0.028	5.22
0.00102	80	0.064	0.022	5.22
0.00102	96	0.054	0.019	5.22
0.00102	48	0.107	0.039	5.22
0.00041	48	0.176	0.025	5.22
0.00064	48	0.150	0.033	5.22
0.00081	48	0.131	0.037	5.22
0.00127	48	0.079	0.035	5.22
0.00160	48	0.042	0.023	5.22
0.00102	48	0.107	0.039	5.22
0.00160	16	0.107	0.012	5.07
0.00127	32	0.107	0.030	5.04
0.00064	64	0.107	0.024	5.05
0.00041	80	0.107	0.015	5.28

Table 3.3 Beam Geometries

Transition Between Face Yielding, Face Wrinkling and Core Shear

$W = 1.55 \text{ N}$ $l = 0.5 \text{ m}$ $b = 0.025 \text{ m}$

$t_{opt} = 0.00324 \text{ m}$ $c_{opt} = 0.173 \text{ m}$ $\rho_{c_{opt}} = 48 \text{ kg/m}^3$ $P/bl = 0.199 \text{ MN/m}^2$

$t \text{ (m)}$	$\rho_c \text{ (kg/m}^3)$	$c \text{ (m)}$	$P/bl \text{ (MN/m}^2)$	$W \text{ (N)}$
0.00324	48	0.173	0.199	1.55
0.00324	16	0.517	0.155	1.55
0.00324	32	0.258	0.164	1.55
0.00324	64	0.129	0.144	1.55
0.00324	80	0.103	0.115	1.55
0.00324	96	0.086	0.096	1.55
0.00324	48	0.173	0.199	1.55
0.00162	48	0.217	0.122	1.55
0.00256	48	0.191	0.168	1.55
0.00408	48	0.149	0.176	1.55
0.00508	48	0.120	0.141	1.55
0.00640	48	0.083	0.098	1.55
0.00324	48	0.173	0.199	1.55
0.00812	16	0.173	0.038	1.51
0.00508	32	0.173	0.110	1.52
0.00164	64	0.173	0.193	1.63

Table 3.3 Beam Geometries

Transition Between Face Yielding and Core Shear - Face Yielding Only

$W = 3.12 \text{ N}$ $l = 0.5 \text{ m}$ $b = 0.025 \text{ m}$

$t_{opt} = 0.00926 \text{ m}$ $c_{opt} = 0.136 \text{ m}$ $\rho_{opt} = 96 \text{ kg/m}^3$ $P/bl = 0.444 \text{ MN/m}^2$

t (m)	ρ (kg/m ³)	c (m)	P/bl (MN/m ²)	W (N)
0.00926	96	0.136	0.444	3.12
0.00926	48	0.273	0.322	3.12
0.00926	64	0.205	0.374	3.12
0.00926	80	0.164	0.321	3.12
0.00926	128	0.102	0.321	3.12
0.00926	192	0.068	0.214	3.12
0.00926	96	0.136	0.444	3.12
0.00164	96	0.242	0.137	3.12
0.00256	96	0.229	0.202	3.12
0.00408	96	0.208	0.292	3.12
0.00640	96	0.175	0.385	3.12
0.00812	96	0.151	0.422	3.12
0.01016	96	0.122	0.426	3.12
0.01272	96	0.086	0.291	3.12
0.00926	96	0.136	0.444	3.12
0.01932	16	0.136	0.030	3.46
0.01272	64	0.136	0.248	3.17
0.01016	80	0.136	0.348	3.02
0.00640	128	0.136	0.299	3.19

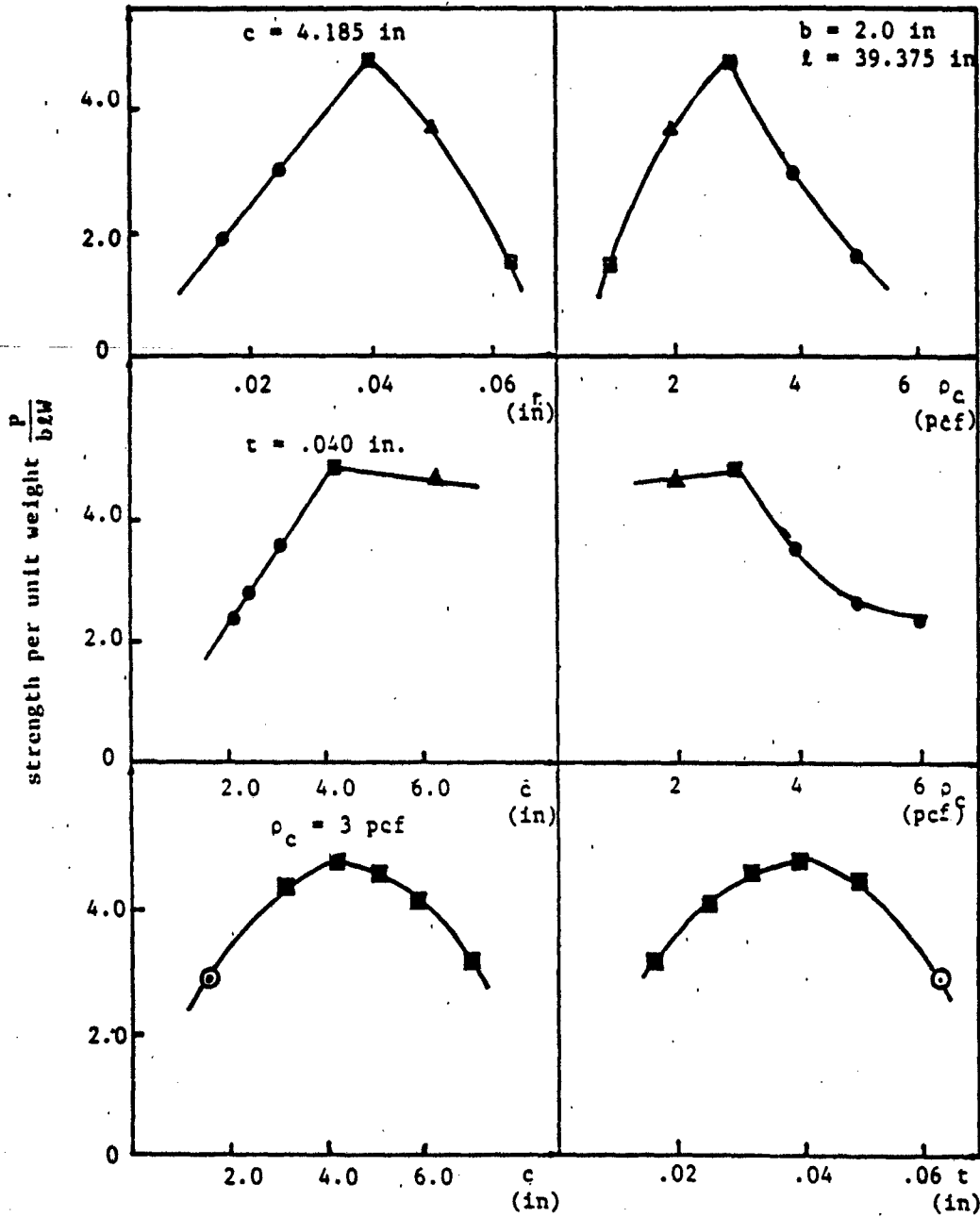


Figure 3.4a Sandwich beams designed for the same weight but different strengths. The optimum beam fails by simultaneous face yielding and face wrinkling; it has $P/bW = 0.039 \text{ MN/m}^2$ and a weight of 3.22 N or 1.17 lb. The failure modes of the other beams are: ● face yielding; ▲ face wrinkling; □ core shearing; and ⊙ simultaneous face yielding, face wrinkling and core shearing.

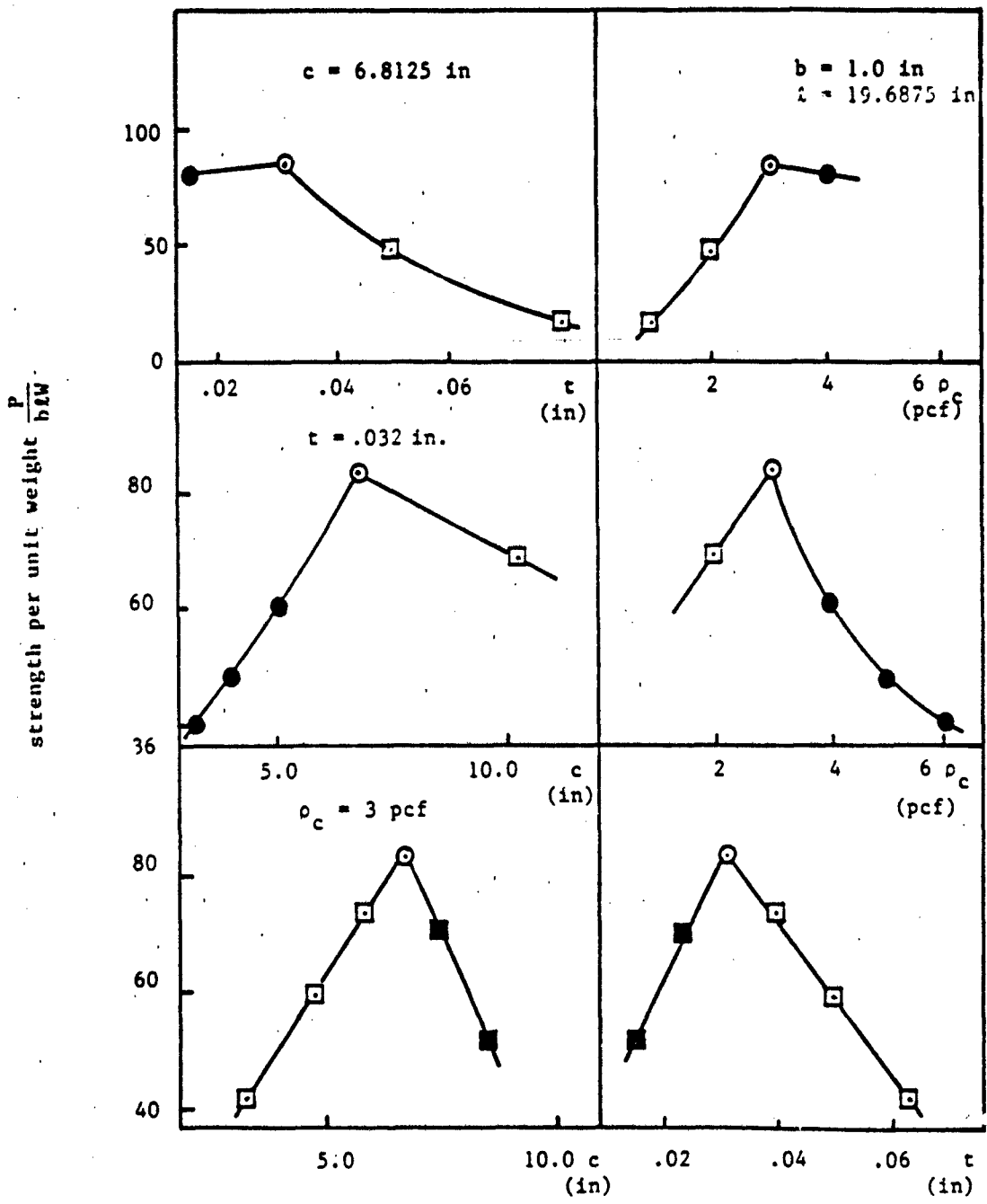


Figure 3.4b) Sandwich beams designed for the same weight but different strengths. The optimum beam fails by simultaneous face yielding, face wrinkling and core shearing; it has $P/bI = 0.199 \text{ MN/m}^2$ and a weight of 1.55 N or 0.35 lb. The failure modes of the other beams are: ● face yielding; ▲ face wrinkling; □ core shearing; and ■ simultaneous face yielding and face wrinkling.

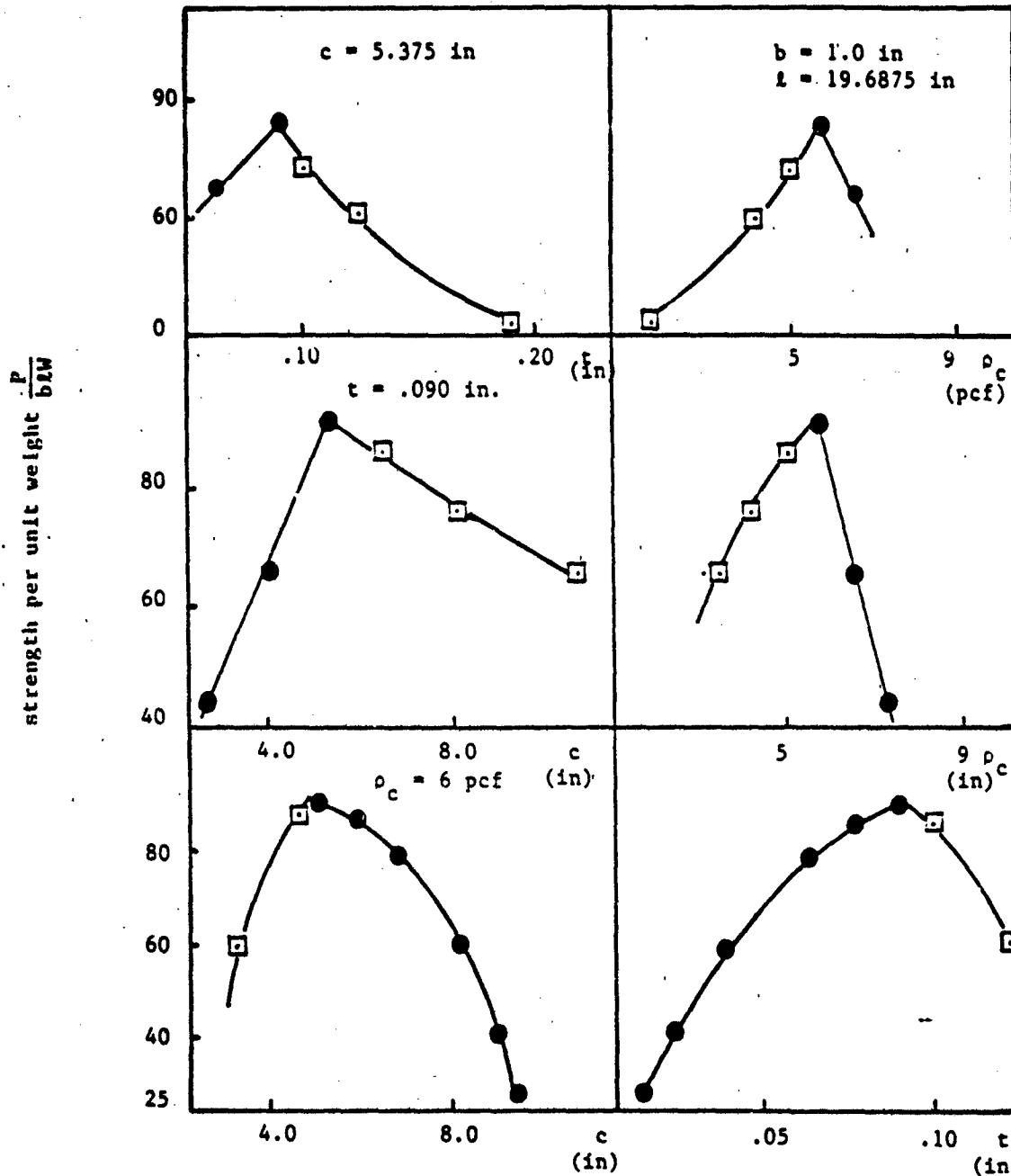


Figure 3.4 c) Sandwich beams designed for the same weight but different strengths. The optimum beam fails by face yielding; it has $P/bI = 0.444 \text{ MN/m}^2$ and a weight of 3.12 N or 0.70 lb. The failure modes of the other beams are: \blacksquare face yielding and face wrinkling; \bullet face yielding; \blacktriangle face wrinkling; \square core shearing; and \circ simultaneous face yielding, face wrinkling and core shearing.

mode maps, showing the transitions between modes were also found to describe the experimental results well; the results are shown in Fig. 3.5 and 3.6. These results, along with the plots shown in Fig. 3.4 indicate that the analysis outlined above will indeed give the minimum weight design of a sandwich beam of a given strength. In the original proposal we suggested performing another set of experiments to confirm the optimization analysis; to do this a series of beams like those given in Table 3.3 would be required. The results of the previous tests [4] indicate that the failure equations developed previously, and used in the analysis here, give the expected failure loads and modes for the beams; the set of tests we originally proposed would only duplicate these results. Consequently, we decided not to pursue the testing of the sandwich beams further. Instead of the originally planned tests, we began work on another aspect of designing sandwich panels: that of predicting the creep behaviour of sandwich panels made with a foam core which creeps.

3.3 Conclusions

The values of the face and core thicknesses and of the core density which minimize the weight of a sandwich beam of a given strength have been found. The analysis has been presented for the case of a sandwich beam with aluminum faces and a rigid polyurethane foam core loaded in three point bending; the method can easily be applied to other face and core materials and other

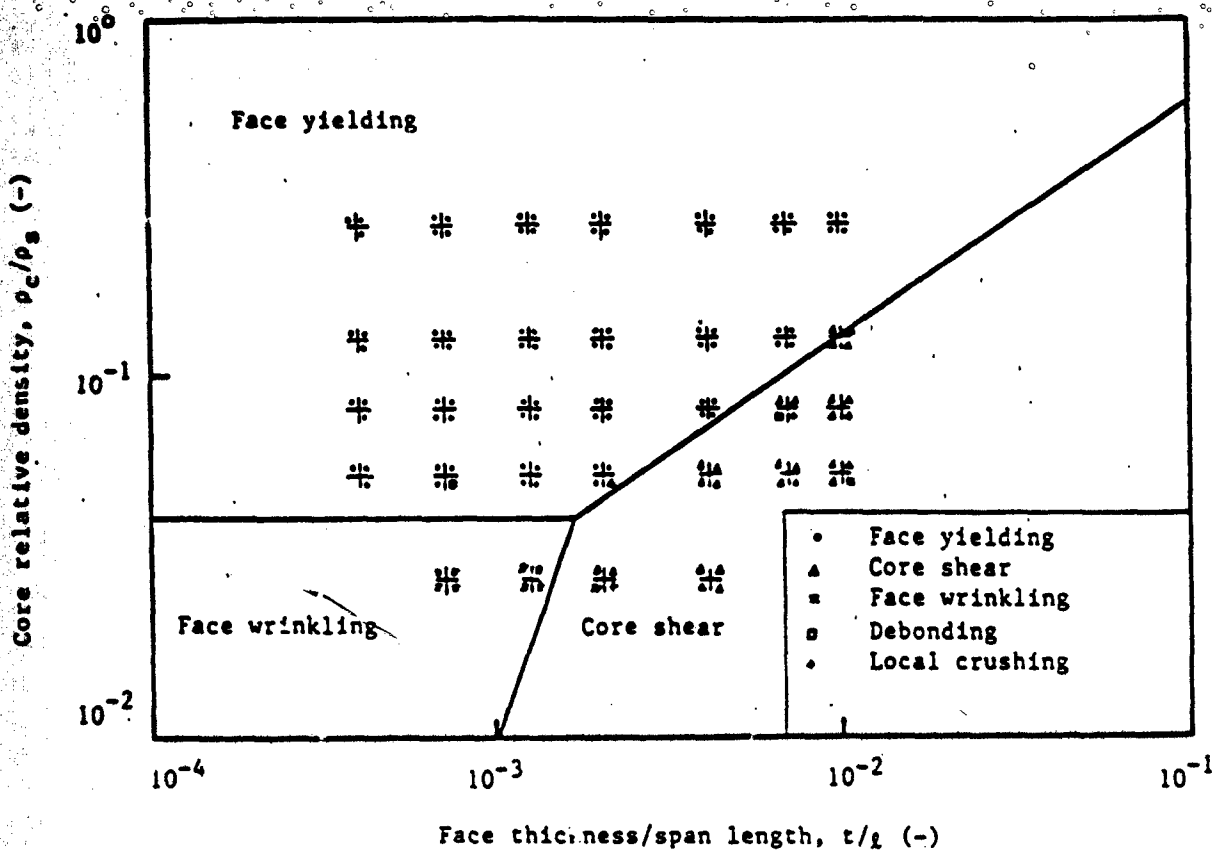


Fig. 3.5 Experimental results of sandwich beams tested in three point bending, plotted on a failure mode map. The beams were 1" wide and had a core thickness of 1". The measured failure modes agree well with those predicted by the map; in particular, the transitions between modes are well predicted.

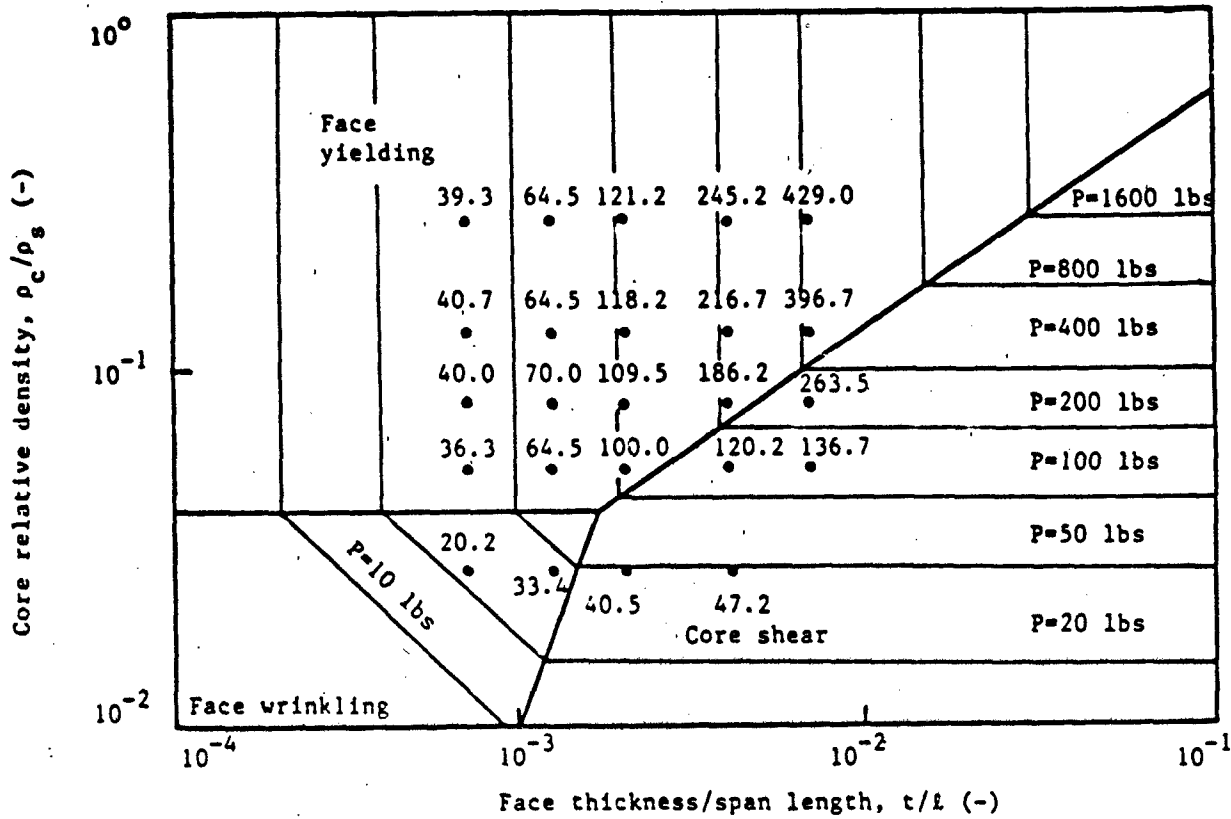


Fig. 3.6 The results of Fig. 3.5 plotted using the measured strengths. For the purposes of comparison, the theoretical strength contours have been superimposed on the map; the agreement is good.

loading conditions. For strengths per unit width and length, P/bl , of less than 0.107 MN/m^2 , the minimum weight beam fails by simultaneous face yielding and face wrinkling; for P/bl between 0.107 and 0.315 MN/m^2 , it fails by simultaneous face yielding, face wrinkling and core shearing; and for P/bl greater than 0.315 MN/m^2 , it fails by simultaneous face yielding and core shearing. For a given required strength of beam, P , span, l , and width, b , the optimum values of face thickness, t , core thickness, c , and core density, ρ_c , can be found from Fig. 3.3, while the minimum weight itself can be read from Fig. 3.2. The values of core density which minimize weight also optimize the thermal performance of the panel.

3.4 References

1. Gibson, L.J., Ashby, M.F., Schajer, G.S. and Robertson, C.I. (1982) Proc. R. Soc. Lond. A382, 25.
2. Gibson, L.J. and Ashby, M.F. (1982) Proc. R. Soc. Lond. A382, 43.
3. Maiti, S.K., Gibson, L.J. and Ashby, M.F. (1984) Acta Met. 32, 1963.
4. Triantafillou, T.C. and Gibson, L.J. (1987) Mat. Sci. and Eng.

4. Creep of Sandwich Panels

4.1 Introduction

At and above their glass transition temperature polymers show slow, permanent, time-dependent deformations, or creep. For many polymers the glass temperature is near room temperature (Table 4.1) making creep an important consideration in the design of sandwich panels using polymeric foam cores. Metals and ceramics creep, too, though the rate of creep is significant only when the temperature is greater than about one third of their melting temperature. In this part of the project, our goal is to describe the creep of a sandwich panel with a polymeric foam core which creeps with time. We plan on first modelling the creep of a foam under constant load and then using the model to describe the resulting creep of the panel. To date, we have reviewed the literature on models for creep in polymers and foams and have done some preliminary calculations on calculating the creep of a sandwich panel with a creeping core. We plan on continuing this work in the next year of the contract.

4.2 Models for Creep in Polymers and Foams

Several models exist for the creep of solid polymers. The simplest are the linear spring-dashpot models: the Maxwell element, consisting of a spring and a dashpot in series; the Voigt element, a spring and dashpot in parallel; and the Burger body, a Maxwell element in series with a Voigt element. The behaviour of each of these elements is described in many texts, see McClintock and Argon [1], for instance. Linear

Table 4.1 The Glass Transition Temperature for Some Common Polymers

Polymer	Glass Temperature (°C)
Thermoplastics	
Polyethylene	20
Polypropylene	-20
Polystyrene	100
Polyvinyl chloride	80
Polymethylmethacrylate	100
Nylons	70
Thermosets	
Epoxies	110
Polyesters	70

creep, for which superposition of stress is valid (e.g. a doubling of stress results in a doubling of the strain at a given time) can be modelled using some combination of these elements. In practice, most polymers do not exhibit linear creep and more refined models are required to describe their behaviour. The three most common descriptions of non-linear creep in polymers are: power-law method, the arc-sinh method and the multiple integral method. Spring dashpot models with non-linear springs and dashpots are also sometimes used.

A plot of creep strain against time often shows three regimes: primary creep, in which the creep strain-rate decreases with time; secondary creep, for which the creep strain-rate is constant; and tertiary creep, for which the creep strain-rate increases with time. Materials with a constant, steady-state secondary creep strain-rate can be described by power law creep according to:

$$\frac{\dot{\epsilon}}{\dot{\epsilon}_0} = \left(\frac{\sigma}{\sigma_0}\right)^n$$

and

$$\dot{\epsilon}_0 = A \exp(-Q/RT)$$

where $\dot{\epsilon}$ is the secondary creep strain-rate, A is a constant, Q is the activation energy for the creep process (a material property), R is the universal gas constant, T is the temperature, σ is the applied stress, σ_0 is a material property and n is

another material property. If the duration of the load is large then the primary creep strains are small compared to the secondary ones and this equation gives a good prediction of the total creep strain. The secondary creep strain-rate of a wide range of metals and ceramics can be described using this equation; it is less commonly used for polymers. Gibson and Ashby have shown that a foam made from a solid cell wall material that obeys power law creep should creep according to [2]:

$$\frac{\dot{\epsilon}^*}{\dot{\epsilon}_{0s}} = \frac{C_9}{n_s + 2} \left\{ \frac{C_{10} (2n_s + 1)}{n_s} \frac{\sigma}{\sigma_a} \right\}^{n_s} \left(\frac{\sigma_s}{\sigma^*} \right)^{\frac{3n_s + 1}{2}}$$

where the superscript * refers to the foam property and the subscript s refers to the solid cell wall property. C_9 and C_{10} are constants which can be determined by considering the two limits of plastic collapse (for which $n_s = \infty$ and $\sigma_{0s} = \sigma_{ys}$) and of linear elasticity (for which $n_s = 1$, $\frac{\sigma}{\epsilon} = E^*$ and $\frac{\sigma_{0s}}{\epsilon_{0s}} = E_s$). We find $C_9 = 0.6$ and $C_{10} = 1.7$. Although both polymer and metal foams have been tested in the creep range, the data are not complete enough to allow a test of the above equation [3-6].

Polymers which do not have a constant, steady-state creep strain-rate can be described in two ways: by the arc sinh method or the multiple integral method. Both are essentially curve fitting techniques. In the arc sinh method, the creep strain is given by [7]:

$$\epsilon = \epsilon'_0 \sinh\left(\frac{\sigma}{\sigma_e}\right) + m't^n \sinh\left(\frac{\sigma}{\sigma_m}\right)$$

where ϵ is the creep strain, σ is the applied stress, t is time, and ϵ_0 , m , n , σ_0 , and σ_m are material constants which are found empirically from a series of creep tests for different levels of applied stress. The above equation can be used to calculate the creep strain of a beam, and hence a foam, made from a material following arc sinh creep. This remains to be done.

Green and Rivlin [8] and Pipkin [9] have shown that the nonlinear creep behaviour of polymers may be expressed as the sum of multiple integrals up to the fifth order. To determine the 27 material constants for the multiple integral representation of creep behaviour under multiaxial stresses the results of three tension tests, two torsion tests and two tests under combined tension and torsion of a thin walled tube are necessary. Brown and Sidebottom [10], in comparing the accuracy of the arc sinh theory and the multiple integral theory found that although the multiple integral theory was more complex, it was no better at predicting creep strains of polyethylene under simple tension, compression or torsion. Because of this, we will not consider the multiple integral theory further.

Little data for the creep of foams exists. The most complete study is that of Nolte and Findley [11] who measured the creep response of both solid and foamed polyurethane under simple tension, compression and torsion and under combined tension and torsion. They used the multiple integral representation to

predict the creep of the solid polyurethane and found that the creep of the foam could be predicted by multiplying the solid creep strains by the ratio of the Young's modulus of the foam to that of the solid.

4.3 Future Work

Creep of foams

Creep tests at different stress levels of foams of different relative densities and of the solid polymer from which they are made are required to determine which creep theory to use to describe the creep of a polymeric foam core and to measure the material properties required for the use of the creep law. In sandwich beams with a creeping foam core, the core may be subject to either simple shear stresses or combined axial and shear stresses; the creep tests of foams under both loading conditions will be necessary to predict the creep of sandwich beams.

Creep of sandwich beams

The elastic deflection of a sandwich beam is the sum of the bending deflection of the beam, which depends on the overall flexural rigidity of the beam, and of its shear deflection, which depends on the shear rigidity of the core. We propose first to analyze the creep of a sandwich beam in which the foam core creeps but faces do not (eg. a beam made with a polyurethane foam core with aluminum faces). Creep tests on sandwich beams with aluminum faces and polyurethane cores will be performed to

compare the analysis with creep data. If the analysis for a creeping core is satisfactory, then the analysis will be extended to examine the problem of a sandwich beam made with both faces and a core that creeps (as in, for instance, a sandwich beam made with wood faces and a foam core). Again, creep tests on sandwich beams with wood faces and a polyurethane foam core will be performed to compare the analysis with creep data. It is hoped that the analysis will suggest design methods which minimize the creep of a sandwich beam under constant load.

4.1 References

1. McClintock, F. and Argon, A. (1966) The Mechanical Behaviour of Materials, Addison Wesley.
2. Gibson, L.J. and Ashby, M.F. (1988) The Structure and Properties of Cellular Solids, Pergamon.
3. Brown, W.B. (1960) Plastics Progress p. 149.
4. Hart, G.M., Balazs, C.F., and Clipper, R.B. (1973) J. Cell. Plast. 9, 139.
5. Thornton, P.H. and Magee, C.L. (1975) Met. Trans. 6A, 1801.
6. Campbell, G.A. (1979) J. Appl. Poly. Sci. 24, 709.
7. Findley, W.N. and Khosla, G. (1956) SPE Journal, December, 1956, 20.
8. Green, A.E. and Rivlin, R.S. (1960) Archive for Rational Mechanics and Analysis 1, 387.
9. Pipkin, A.C. (1964) Reviews of Modern Physics 36, 125.
10. Brown, R.L. and Sidebottom, O.M. (1971) Trans. Soc. Rheology 15, 3.
11. Nolte, K.G. and Findley, W.N. (1970) J. of Basic Engineering, ASME, March, 1970, p 105.

5. Conclusions

From this study of optimum design methods for structural sandwich panels we conclude the following.

(a) Debonding

The equations derived for the debonding load describe the experimental data well. Debonding is only a problem when there is a preexisting crack larger than twice the depth of the core, which is unlikely to be the case.

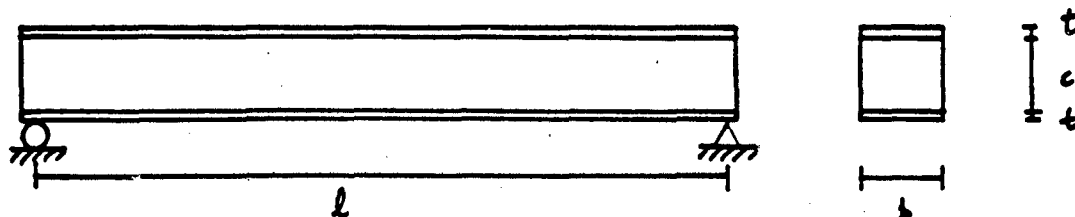
(b) Minimum weight design of sandwich beam of a given strength

Failure mode maps can be used to find the critical failure mode for any given strength of sandwich beam of known width and span. The analysis gives the face and core thicknesses and the core density which minimize the weight of the beam for any given strength; the results are summarized in Fig. 3.3 and 3.4. The optimum core density for a sandwich beam with aluminum faces and a polyurethane foam core loaded in three point bending is between 3 and 4.5 pounds per cubic foot for P/bl up to 100 psi; it is interesting to note that the thermal conductivity of foams is lowest at this density so that this optimizes the thermal performance of the panel also.

(c) Creep of sandwich beams

The initial literature review of models for creep in solid polymers and foams is complete. We propose continuing work on creep of sandwich beams in the second year of the project. Specifically, we propose measuring creep in foams and in sandwich beams made using those foams.

APPENDIX - LIST OF SYMBOLS



Sandwich beam geometry

- b width
- c core thickness
- l span
- t face thickness
- W total weight of the beam
- g acceleration due to gravity
- W/g total mass of the beam

Loading configuration

- C_1 = a constant relating the product of the applied load, P, and the span, l, to the maximum moment acting on the beam
 $= Pl/M_{max}$
- C_2 = a constant relating the applied load, P, to the maximum shear stress in the beam
 $= P/bc\tau_c$

Material Properties

- ρ_f density of the face material
- E_f Young's modulus of the face material
- σ_{yf} yield strength of the face material
- ρ_c density of the foam core
- E_c Young's modulus of the foam core
- G_c shear modulus of the foam core
- σ_{ct} tensile yield strength of the foam core
- σ_{cc} compressive yield strength of the foam core
- τ_c^* shear yield strength of the foam core
- ρ_s density of the solid from which the core is foamed
- E_s Young's modulus of the solid from which the core is foamed
- σ_{ys} yield strength of the solid from which the core is foamed

The following relationships apply to the foam core and the solid from which it is foamed:

$$E_c / E_s = C_3 (\rho_c / \rho_s)^A$$

$$\tau_c^* / \sigma_{ys} = C_4 (\rho_c / \rho_s)^B$$

$$\sigma_{ct} / \sigma_{ys} = C_5 (\rho_c / \rho_s)^C$$

$$\sigma_{cc} / \sigma_{ys} = C_6 (\rho_c / \rho_s)^F$$